Molecular origin of the anisotropic dye orientation in emissive layers of organic light emitting diodes

Molecular origin of the anisotropic dye orientation in emissive layers of organic light emitting diodes

Pascal Friederich, Reinder Coehoorn, Wolfgang Wenzel*

P. Friederich, W. Wenzel

Institute of Nanotechnology, Karlsruhe Institute of Technology, Hermann-von-Helmholtz-Platz 1, 76344 Eggenstein-Leopoldshafen, Germany

E-mal: wolfgang.wenzel@kit.edu

R. Coehoorn

Department of Applied Physics and Institute for Complex Molecular Systems, Eindhoven University of Technology, 5600 MB Eindhoven, Netherlands

Keywords: Organic electronics, Organic light emitting diodes, Organic semiconductors, Outcoupling efficiency, Molecular simulations

Molecular orientation anisotropy of the emitter molecules used in organic light emitting diodes (OLEDs) can give rise to an enhanced light-outcoupling efficiency, when their transition dipole moments are oriented preferentially parallel to the substrate, and to a modified internal quantum efficiency, when their static dipole moments give rise to a locally modified internal electric field. Here, the orientation anisotropy of state-of-the-art phosphorescent dye molecules is ivestigated using a simulation approach which mimics the physical vapor deposition process of amorphous thin films. The simulations reveal for all studied systems significant orientation anisotropy. Various types are found, including a preference of the static dipole moments to a certain direction or axis. However, only few systems show an improved outcoupling efficiency. The outcoupling efficiency predicted by the simulations agrees with experimentally reported values. The simulations reveal in some cases a significant effect of the host molecules, and suggest that the driving force of molecular orientation lies in the molecule-specific van der Waals interactions of the dye molecule within the thin film surface. The electrostatic dipole-dipole interaction slightly reduces the anisotropy. These findings can be used for the future design of improved dye molecules.

1. Introduction

In 2011, Schmidt et al.[1] showed that there can exist an anisotropy in the orientation distribution of phosphorescent dye molecules in organic light emitting diodes manufactured by vapor deposition. The orientation anisotropy of certain emitters leads to a preferential orientation of the molecular transition dipole moment vectors (TDV) parallel to the thin film plane.[2-14] The optical power is emitted mainly in directions perpendicular to the transition dipole moment, making an in-plane orientation of the TDV favorable for obtaining a high light-outcoupling efficiency. The TDV orientation anisotropy is usually quantified in terms of an orientation descriptor Θ which is defined as the average of the square of the cosine of the angle between the TDV and the growth direction. For a system with only horizontal or vertical dipoles, Θ would be the fraction of vertical dipoles. The value of Θ is 1/3 for a completely isotropic orientation distribution and smaller than 1/3 in the case of preferential in-plane orientation. While there have been several experimental reports of an orientation-induced variation of the outcoupling efficiency,[1, 7, 11, 12] the microscopic origin and the driving force of the molecular orientation anisotropy are still unclear, which prevents a systematic design of more efficient dye materials. Further-

more, developing improved understanding of the orientation anisotropy is also important when the emitter molecules have a large static dipole moment. Static dipole orientation can lead to a significant modification of the internal electrostatic field, as is known from the observation of a giant surface potential (GSP) effect,[15-17] which influences the transport and density distribution of electrons and holes in the thin film, and hence the internal quantum efficiency.

Here we present an atomistic simulation approach for calculating the anisotropic dye orientation distribution in mixed host-guest systems as used in the emissive layers of OLEDs. We demonstrate its predictive power by reproducing the experimentally measured Θ values of three iridium complexes embedded in 4,4′-bis(N-carbazolyl)-1,1′-biphenyl (CBP), discussed by Jurow et al.[7] A microscopic analysis of the various intermolecular interactions affecting the molecular orientation indicates that the main driving force is the van der Waals interaction between the molecules at the surface. The electrostatic dipole-dipole interaction is found to slightly reduce the anisotropy. We include in our study eight iridium-based emitter molecules, with a wide range of static dipole moments, embedded in three different host materials including the polar material diphenyl-4-triphenylsilylphenyl-phosphineoxide (TSPO1). First, the overall static dipole orientation distribution and the short-range correlations between the static dipole moment orientations are analyzed. Subsequently, we calculate for all emitter molecules the transition dipole moment axis direction using time-dependent density functional theory (TDDFT), and analyze the effect of the orientation anisotropy found on the Θ values of all systems studied.

2. Vapor deposition simulation

To simulate the physical vapor deposition process on an atomistic level, we use a Monte Carlo based simulated annealing (SA) protocol which sequentially deposits molecules on an amorphous film.[18] During the deposition of each molecule, the simulation temperature undergoes 10 SA cycles from artificially high temperatures (4000 K) to room temperature (300 K). The molecular energies (E_{total}) are evaluated using a force field which incorporates the Lennard-Jones interaction energy (E_{LJ}) describing van der Waals attraction and the Pauli repulsion, the electrostatic interaction ($E_{electrostatic}$) and, to model molecular flexibility, the intramolecular dihedral potential energy ($E_{dihedral}$):

$$E_{\text{total}} = E_{\text{LJ}} + E_{\text{electrostatic}} + E_{\text{dihedral}} \quad \text{(Eq. 1)}$$

The intramolecular degrees of freedom are expressed in terms of dihedral rotations which are parameterised for each type of molecule using semiempirical PM7 calculations.[19, 20] The ground state geometries as well as the electrostatic-potential-fitted partial charges (ESP charges) for the electrostatic force field are calculated using density functional theory (DFT) calculation on a def2-SV(P)/B3-LYP/DFT-D3 level of theory.[21-24] The final states of the sequential SA cycles are accepted or rejected according to the Metropolis Monte Carlo criterion.

3. Transition dipole moment orientation – comparison with experiment

Using the protocol introduced above, we have generated amorphous morphologies of eight mixed host-guest systems. Before presenting a systemic discussion of all simulation results, we first focus, for comparison with experiments performed by Jurow et al.,[7] on the transition dipole moment orientation as obtained for the iridium compounds shown in **Figure 1**, embedded in a matrix of CBP. As in the experiments, we used guest concentrations of 10 and 20 mol%. For each host-guest combination and guest concentration, we generated four morphologies with 850 molecules each, resulting in 6800 molecules per host-guest combination. In order to calculate Θ, we determined the orientation of the TDVs of all emitter molecules in the amorphous films. For that purpose, we used the transition dipole direction assumed by Jurow et al., where the direction of the TDV-axis is in the bppo ligand plane between the Ir-N and the Ir-C bond with an angle to the Ir-N bond of 20°. The simulated and experimental Θ values, which are both included in **Figure 1**, show a fair agreement. We will later re-analyze these results on the basis of a more in-depth analysis of the intramolecular TDV direction and its influence on Θ.

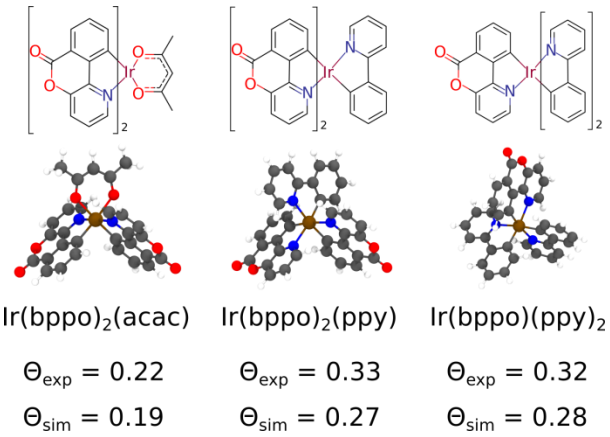

Figure 1. Molecular structure of the iridium-emitters Ir(bppo)₂(acac), Ir(bppo)₂(ppy) and Ir(bppo)(ppy)₂, and experimental and simulated values of the parameter Θ which characterizes the average orientation of the transition dipole moment with respect to the film normal, averaged in films with a 10% and 20% dye concentration. Here bppo, acac and ppy are benzopyranopyridinone, acetylacetonate and 2-phenylpyridinate. The experimental data were taken from Jurow et al.[7].

4. Orientation mechanism – static dipole moment orientation distribution

This fair agreement between the vapor deposition simulation and experimental results motivated us to further study

a variety of state-of-the-art host-guest systems, in order to understand and potentially control the

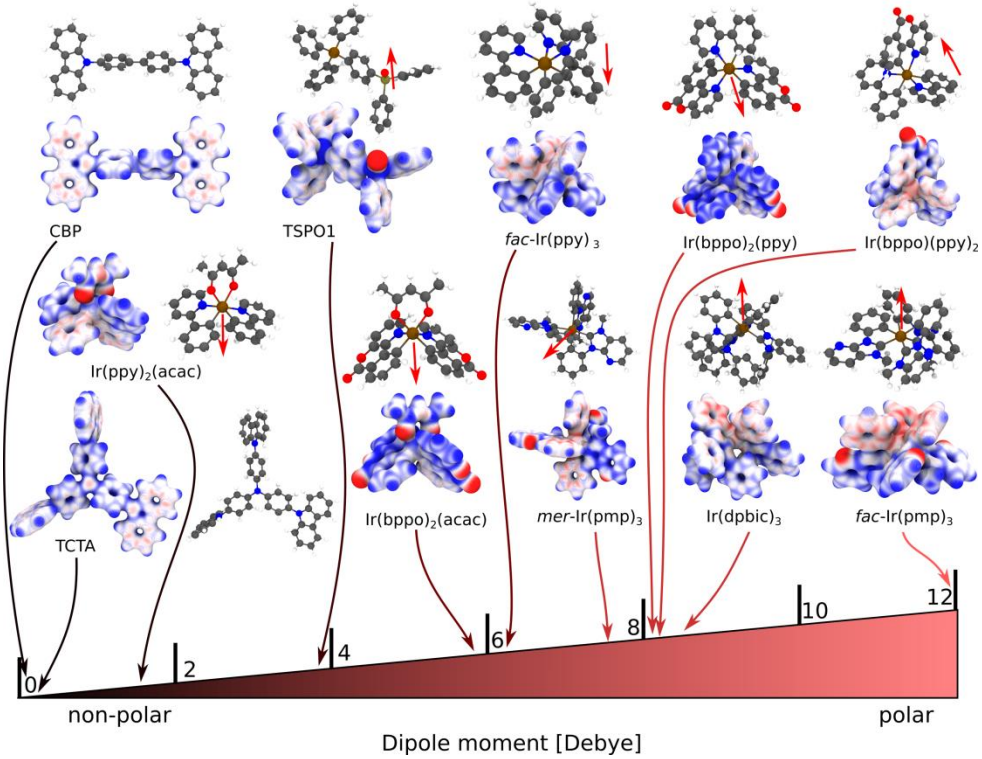

Figure 2. Chemical structures, electrostatic potential on surfaces of constant electron density, and electrostatic dipole moments of all host and dye molecules used in this work. Colors of the atoms: carbon - gray, hydrogen - white, nitrogen - blue, oxygen - red, iridium - brown, silicon - light brown, and phosphorous - yellow. The red arrows indicate the direction of the static dipole moments and point in the direction of the negative pole.

Table 1. Host-guest combinations included in this study, concentrations used for the generation of atomistic morphologies and ensemble-averaged value of the *z*-component of the static dipole moment of the emitter molecules, $\langle \cos \theta_z \rangle$, with θ_z the angle of the static dipole moment with respect to the perpendicular (out-of-the-film, positive *z*) direction.

host	guest	guest concentration *c* [mol%]	mean guest static dipole orientation, $\langle o \rangle \equiv \langle \cos \theta_z \rangle$
CBP	$Ir(bppo)_2(acac)$	20	0.339
CBP	$Ir(bppo)_2(ppy)$	20	0.210
CBP	$Ir(bppo)(ppy)_2$	20	0.040
TSPO1	*fac*-$Ir(pmp)_3$	15	0.034
TCTA	*fac*-$Ir(pmp)_3$	15	0.112
TSPO1	*mer*-$Ir(pmp)_3$	15	0.035
TCTA	*fac*-$Ir(ppy)_3$	6	0.146
TCTA	$Ir(ppy)_2(acac)$	6	0.333

$Ir(dpbic)_3$	-	-	0.105

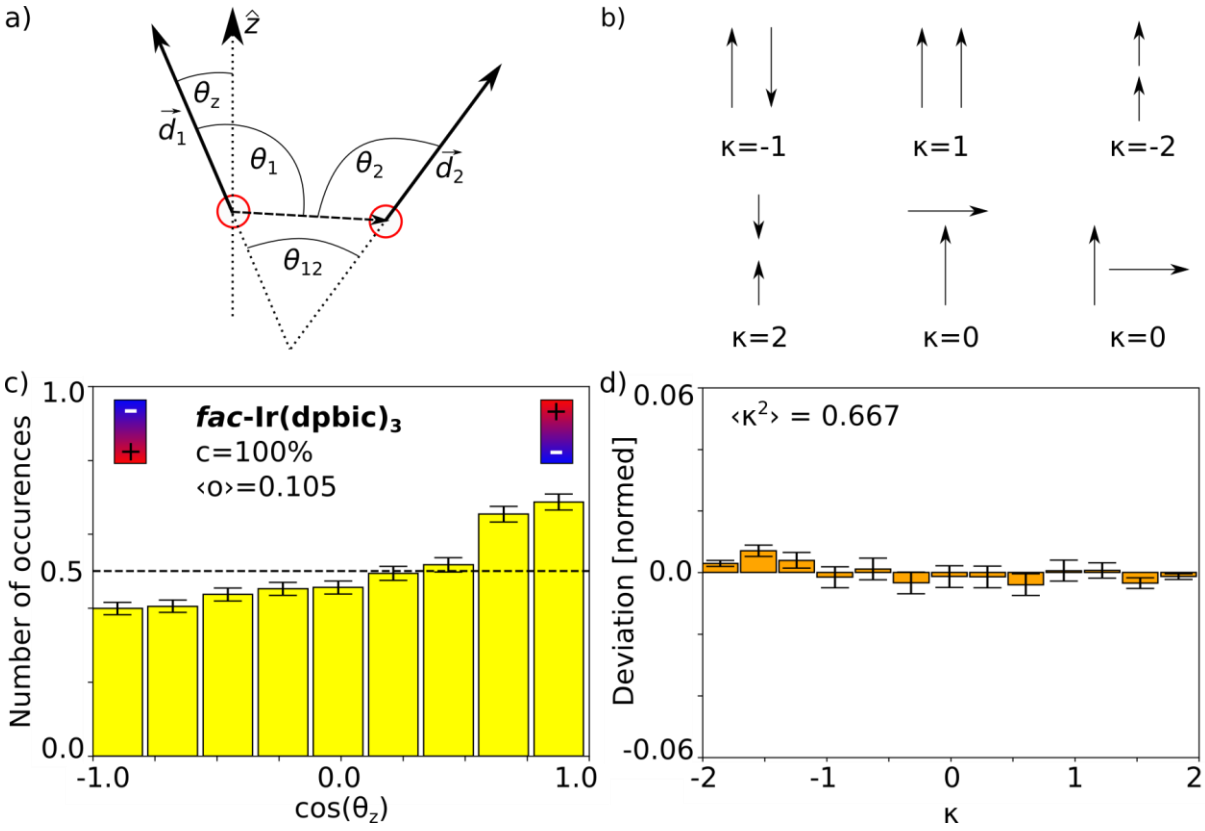

Figure 3. a) Definition of the absolute and relative angles used for the calculation of the prefactor κ in the expression for the dipole-dipole interaction energy. The red circles denote the position of the molecules and the dashed arrow is the vector connecting the two molecules. b) Examples of relative dipole orientations values and the corresponding κ values. c) Distribution of orientations of molecular dipole moments in neat films of $Ir(dpbic)_3$. The dashed line corresponds to a random (isotropic) molecular orientation distribution. d) Deviation of the distribution of κ values of relative dipole orientations in neat films of $Ir(dpbic)_3$ from the distribution of κ values in an isotropic system. Deviations from the dashed line in panel c) and from zero in panel d) are a measure of the global orientation anisotropy and the local orientation correlation, respectively.

orientation of the dye molecules in the film. We will first focus on the dependence of the static dipole moment orientation distribution on the film composition. As no covalent bonds are created or broken during deposition, we analyze the orientation anisotropy in terms of the two non-covalent contributions, i.e. dispersion interactions modelled by the van der Waals potential and electrostatic interactions.

Table 1 gives an overview of all host-guest combinations studied and the guest concentrations employed. Our study includes the blue emitters fac- and mer-tris-(N-phenyl, n-methyl-pyridoimidazol-2-yl)iridium(III) (fac-$Ir(pmp)_3$ and mer-$Ir(pmp)_3$)[5], the widely used green emitter tris[2-phenylpyridinato-C^2,N]iridium(III) ($Ir(ppy)_3$)[25] and the yellowish-green emitter $Ir(ppy)_2(acac)$. As host materials, we included TSPO1 and tris(4-carbazoyl-9-ylphenyl)amine (TCTA). The chemical structures and the electrostatic potentials on isosurfaces of the electron density of these molecules are shown in **Figure 2**. The calculated static dipole moments are given in **Table 2**. The dipole moments of the dye molecules ranges from 1.6 Debye for $Ir(ppy)_2(acac)$ to 11.8 Debye for fac-$Ir(pmp)_3$. This wide range gives us the possibility to analyze the role of dipole-dipole interactions on the orientation anisotropy. If available, a comparison with literature values is included in the table. Deviations can arise due to different functionals, basis-sets or further methodological differences within DFT. We furthermore analyzed the orientation anisotropy in neat films of the hole-conducting and electron-blocking molecule fac-tris(1,3-diphenyl-benzimidazolin-2-ylidene-C,C2')iridium(III) ($Ir(dpbic)_3$).[26, 27]

The shape of the dipole orientation distribution function is described fully by the averages over all emitter molecules of the quantities $[\cos\theta_z]^n$, with θ_z the angle of the static dipole moment vector with respect to the perpendicular (out-of-the-film, positive z) direction and with n = 0, 1, 2, … . The mean static dipole orientations

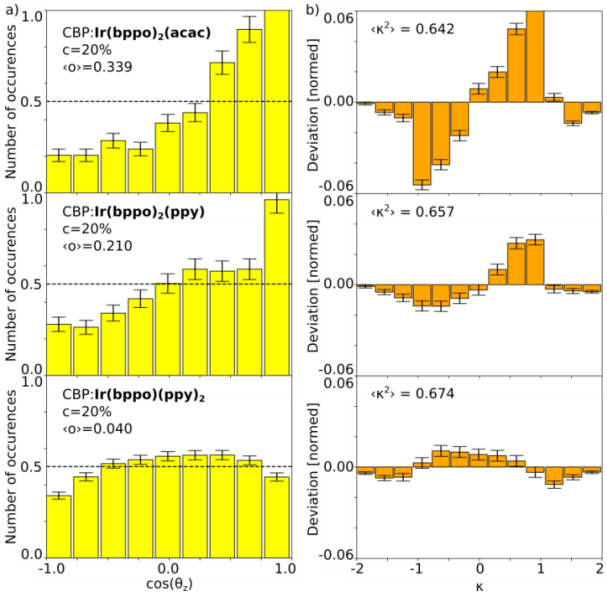

Figure 4. a) Distribution of dipole orientations of Ir(bppo)₂(acac), Ir(bppo)₂(ppy) and Ir(bppo)(ppy)₂ with respect to the z-axis. The dashed line corresponds to a random (isotropic) orientation of the molecules. c is the concentration of the material written in bold letters. b) Deviation of the distribution of κ values of relative dipole orientations of dye-pairs from the distribution of κ values in an isotropic system.

$\langle o \rangle \equiv \langle \cos\theta_z \rangle$ obtained for mixed films with guest concentrations c of 6 mol% and 15 mol% are given in **Table 1**. In the mixed systems, only the iridium dye dipole moments were included, whereas in the case of neat $Ir(dpbic)_3$ films, all dipole moments were taken into account. We find significant deviations from the isotropic expectation value of $\langle o \rangle = 0$, indicating systematic dipole orientation effects in all investigated systems. In all cases, the more positive parts of the molecules are oriented towards the vacuum.

Figure 3c, **4a** and **5a** show for all systems studied the emitter orientation distribution as obtained from the simulations, expressed as the normalized number of occurrences in nine equally large bins of $\langle \cos\theta_z \rangle$. For neat $Ir(dpbic)_3$ films (**Figure 3c**), we observe a significant deviation from an isotropic orientation (dashed line), with an excess of molecules oriented with their partially positively charged pole towards the vacuum. The mean orientation is $\langle o \rangle = 0.105$. For the heteroleptic iridium complexes incorporating one single acac or ppy ligand ($Ir(bppo)_2(acac)$, $Ir(bppo)_2(ppy)$ and $Ir(ppy)_2(acac)$), we observe a similar orientation anisotropy (**Figure 4a** and 5a). These relatively small partially positively charged groups point with a higher probability away from the surface while the van der Waals interaction of the other ligands with the already deposited film reduces the total energy. A similar but more subtle effect occurs for TCTA containing fac-$Ir(ppy)_3$, whose dipole moment arise from the asymmetry of the positions of the partially positively

Table 2. Static dipole moments of the host and guest molecules, as obtained from DFT.

	Dipole moment [Debye] (this study)	Dipole moment [Debye] (literature)
Ir(bppo)2(acac)	5.8	
Ir(bppo)2(ppy)	8.2	
Ir(bppo)(ppy)2	8.1	
fac-Ir(pmp)3	11.8	17.2 5
mer-Ir(pmp)3	7.5	10.8 5
fac-Ir(ppy)3	6.2	6.3 4
Ir(ppy)2(acac)	1.6	1.9 4
Ir(dpbic)3	8.4	
TSPO1	3.8	
TCTA	0.1	
CBP	0.0	

charged nitrogen atoms. The excess electron density on the opposite side of the molecule increases the van der Waals attraction with the surface, leading to a preferential orientation of fac-$Ir(ppy)_3$ with the nitrogen atoms pointing towards the vacuum (**Figure 4a**). In case of the more disc-shaped molecule fac-$Ir(pmp)_3$, the two possible orientations which optimize van der Waals interaction with the surface lead to an approximately equal preference of the dipole orientation in the +z or -z directions. We therefore observe a U-shaped distribution of dipole orientations and a lack of molecules with an in-plane orientation of their electrostatic dipole moments (**Figure 5a**).

We do not observe a significant dependence of the orientation anisotropy on the dye concentration. That may be seen from **Figure 6a**, which gives an overview of the simulated net orientation of guest dipole moments in six systems. In order to be able to evaluate the net dye orientation with sufficient accuracy, we generated in total 20 (10) morphologies for each host-dye system at dye concentrations

of 3 mol% (6 mol%), corresponding to a total number of ~25000 (~12500) molecules per host-dye concentration or ~1000 dye molecules. The large statistical uncertainty makes it hard to extract conclusive and quantitative information. However, we nevertheless cannot exclude a weak concentration dependence of the net orientation. This weak concentration dependence indicates that dipole-dipole interactions, which would counteract the development of a large net perpendicular dipole orientation, do actually not play a dominant role.

5. Short-range static dipole orientation correlations

The simulation results presented so far indicate that for these systems the anisotropy of the van der Waals interaction for molecules at the surface is the dominant interaction effect. Nevertheless, dipole-dipole interactions may lead to another effect, which does not appear from the overall orientation distribution function, viz. the development of short-range static dipole moment orientation correlations. Such an effect would influence the electron and hole transport by affecting the highest occupied molecular orbital (HOMO) and the lowest unoccupied molecular orbital (LUMO) levels. The orientation correlation can arise due to the angular dependence of the dipole-dipole interaction energy, which is given by

$$E_{\mathrm{dd}} = \kappa \frac{d_1 d_2}{4\pi\varepsilon_{\mathrm{r}}\varepsilon_0 r^3} , \qquad \text{(Eq. 2)}$$

with ε_0 the vacuum permittivity, ε_{r} the relative permittivity, which is around 3 to 4 for most organic semiconductors, r the distance between the two dipole moments with size d_1 and d_2, and κ a factor which describes their relative orientation:

$$\kappa = \cos\theta_{12} - 3\cos\theta_1 \cos\theta_2 \quad . \qquad \text{(Eq. 3)}$$

The angles θ_1, θ_2 and θ_{12} are defined as depicted in **Figure 3a**. **Figure 3b** shows the value of κ for various cases. For isotropic systems, the mean value of κ is zero and the mean value of κ^2 is ⅔. To analyze the electrostatic interaction between molecules, we have calculated the κ parameter for all dye pairs in the amorphous films. **Figure 3d**, **4b** and **5b** show the deviation from the distribution of κ values from a distribution which can be expected in a completely isotropic system and give the values of $\langle\kappa^2\rangle$. **Figure S1** (Supplementary information) gives the distance-dependence of the κ distributions. The distributions are very close to those expected for isotropic orientations. Only at intermolecular (center-of-mass) distances of about 1.0 – 1.5 nm, $\langle\kappa\rangle$ drops below 0, leading to an overall mean value of κ^2 slightly below ⅔. We thus do not find pronounced short-range orientation correlation effects.

Combining the observations of the last two sections, all observations indicate that short-range Lennard-Jones interactions (the van der Waals attraction and the Pauli repulsion) rather than long-range electrostatic interactions are responsible for the anisotropic dye molecule orientation. The degree of the orientation and the shape of the dipole orientation distribution are mainly determined by the individual shapes of the molecules. The dipole-dipole interaction slightly reduces the net orientation by aligning neighboring molecules in an antiparallel way.

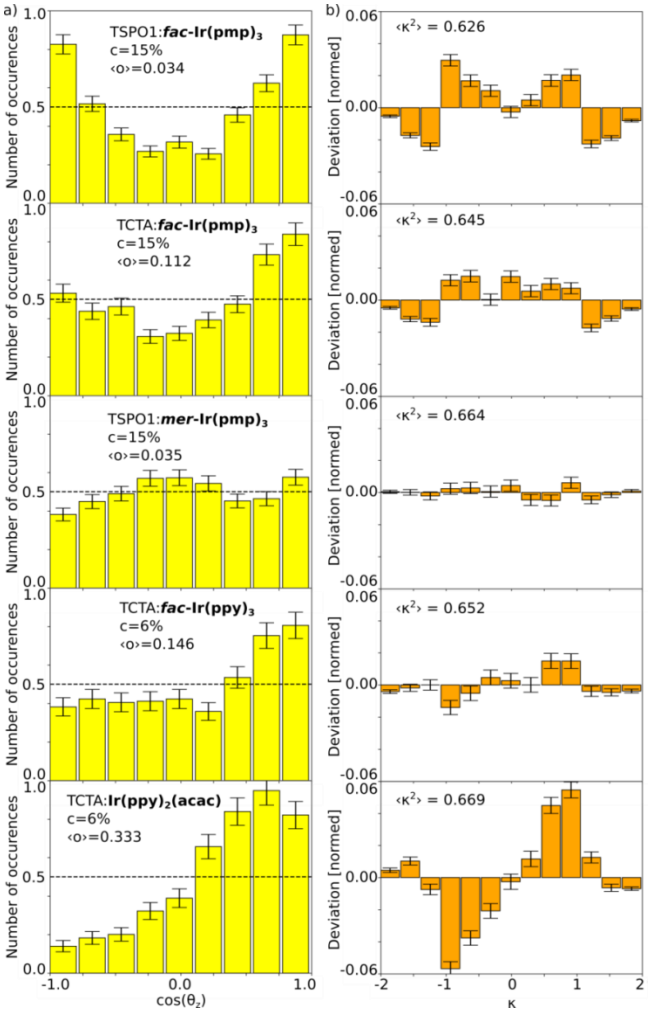

Figure 5. a) Distribution of dipole orientations of fac-Ir(pmp)₃, mer-Ir(pmp)₃, Ir(ppy)₃ and Ir(ppy)₂(acac) with respect to the z-axis. The dashed line corresponds to random (isotropic) orientations of molecules. c is the concentration of the material written in bold letters. b) Deviation of the distribution of κ values of relative dipole orientations of dye-pairs from the distribution of κ values in an isotropic system.

Similar to the findings of Moon *et al.*,[28] we find a rather symmetric distributions of $Ir(ppy)_3$ molecules while $Ir(ppy)_2(acac)$ has a preferential alignment with the ppy ligands pointing towards the substrate. We agree with Lee *et al.*,[29] that the broken symmetry during the growth process is responsible for the orientation of molecules but we go one step further and show that the static dipole moments do not significantly influence the outcoupling efficiency, which means that the orientation of molecules is a

process mainly driven by van-der-Waals interaction between molecules and the substrate.

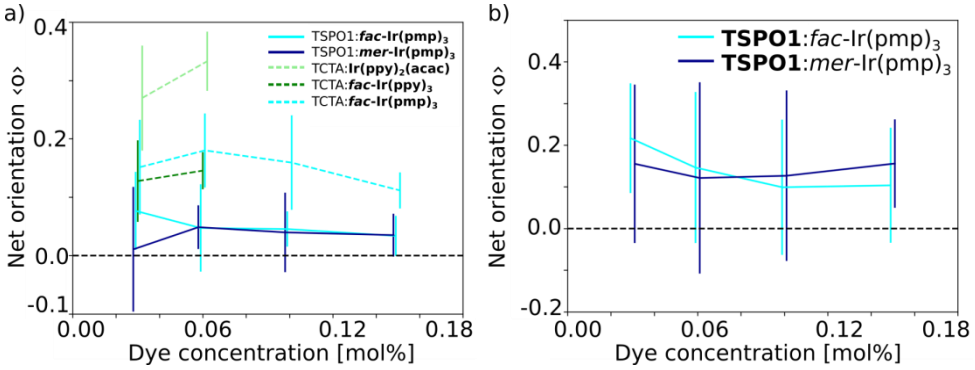

Figure 6. Net orientation <o> of the dipole moments of a) the dye molecules and b) the TSPO1 host molecules, as a function of the dye concentration. *The vertical lines are error bars indicating the statistical uncertainties.*

resulting modified host-guest interaction could be important to the dipole-induced internal electrostatic field and to the guest dipole orientation distribution. In order to study such effects, we have analyzed the orientation anisotropy of TSPO1 host molecules in systems containing fac-Ir(pmp)$_3$ and mer-Ir(pmp)$_3$ as a guest. TSPO1 has a small but non-negligible dipole moment of 3.8 Debye (see **Figure 2**), which mainly arises from the polarity of the phosphine oxide group. For both systems, we observe a distinct anisotropy of the molecular dipoles, which are preferentially parallel to the growth axis (*z*-) direction, as shown in **Figure 7a** and **7b**. A similar distribution was found for the disc-shaped fac-Ir(pmp)$_3$ molecule in TSPO1 (**Figure 5a**). The results in **Figure 7a** indicate that the P=O bond points preferentially in the +*z* or -*z* direction. We attribute that to the large van der Waals interaction of the molecule with the other molecules at the surface when five phenyl rings are in contact with the surface. The P=O bond direction is then orthogonal to the substrate plane. These findings are independent of the dye molecule embedded into TSPO1 and are also rather independent of the dye concentration used.

The resulting net orientation of the TSPO1 dipole moments, with $\langle o \rangle \cong 0.01 - 0.015$ in a wide range of emitter concentrations (see **Figure 6b**), creates an electrostatic background field similar to the giant surface potential effect (GSP) reported by Ishii and coworkers for other organic molecules such as Alq$_3$.[15, 17] The interaction of the dipole moments of the dye molecules with this field might explain the weaker asymmetry in the distribution of fac-Ir(pmp)$_3$ when embedded in TSPO1 ($\langle o \rangle = 0.034$), as compared to fac-Ir(pmp)$_3$ when embedded in TCTA ($\langle o \rangle = 0.112$). As the internal electric fields generated by the orientation of host and guest dipole moments have a considerable effects on the charge distribution and charge dynamics in OLEDs, we suggest to experimentally measure the strength of the surface potential created by the dye molecules in mixed organic layers.

6. Host anisotropy

In systems within which the host has a significant static dipole moment, host molecular orientation and a

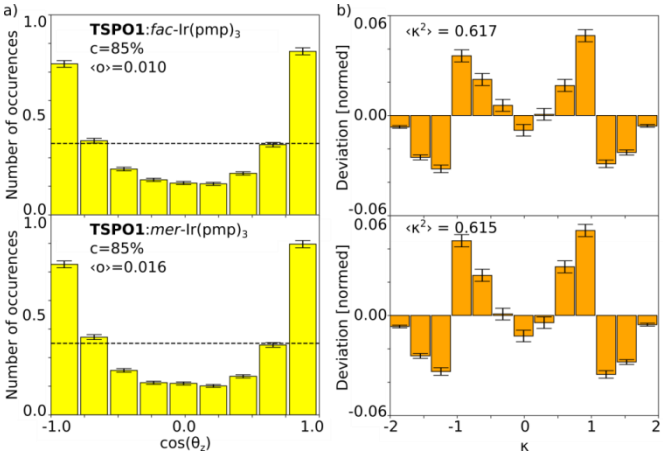

Figure 7. a) Orientation of TSPO1 molecules in mixed TSPO1-dye systems. The dashed line corresponds to random (isotropic) orientations of molecules; c is the concentration of the material written in bold letters. b) Deviation of the distribution of κ values of relative dipole orientations of TSPO1 host-pairs from the distribution of κ values in an isotropic system.

7. Orientation of the transition dipole moments – first principles calculations

After having analyzed the anisotropy of the static dipole orientation distribution for a variety of systems, we return to the subject of the orientation distribution of the emitter transition dipole moments. An issue which has not yet been fully solved is the relationship between the orientation of a specific molecule and the contribution of that molecule to the Θ value. A complicating factor is that each optically active ligand has a TDV. Furthermore, the analysis is affected by uncertainties in the determination of the direction of the TDV in each ligand. The transition dipole

moments associated with metal-to-ligand triplet excitations in the iridium complexes usually point from the iridium center towards the respective ligand. Especially in multi-ligand complexes, a net orientation of molecules does not necessarily lead to a net orientation of the transition dipole moments.

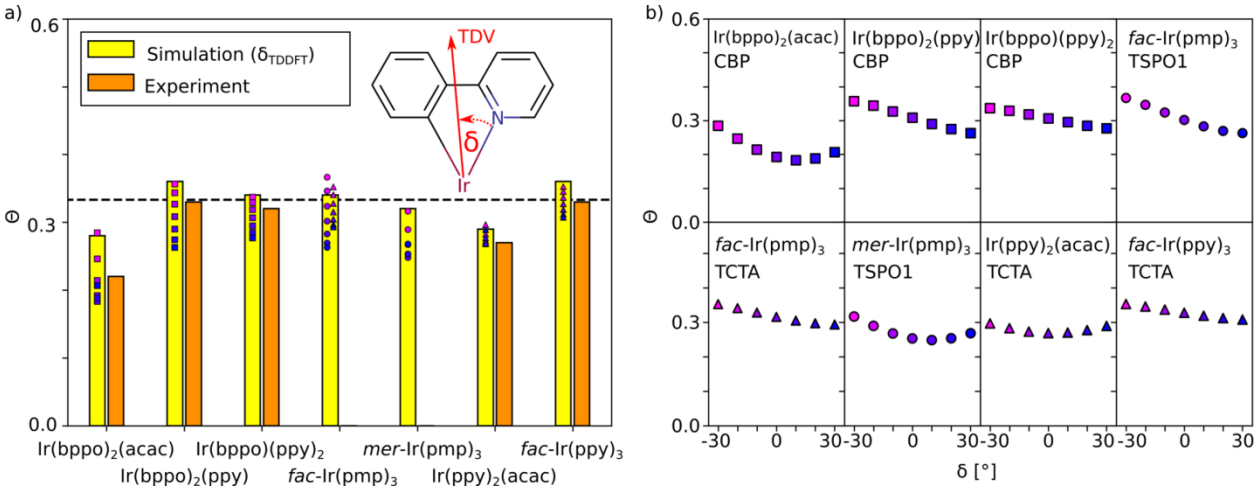

Figure 8. a) Transition dipole orientation parameter Θ as obtained from simulations and experiment,[7, 9, 11] calculated for values of the TDV direction δ in the range -30° to +30° (see inset as well as Figure S2 and Table S1). The yellow bars result from the δ angles obtained from TDDFT calculations. The shape of the symbols indicates the type of host (see panel b)). For Ir(ppy)$_2$(acac) and Ir(ppy)$_3$, the experimental value of Θ = 0.27 was obtained for mixtures with CBP[30], while also higher anisotropies of Θ = 0.23 − 0.24 were reported for the CBP host [9, 31] and for a 1:1 mixed TCTA:B3PYMPM host.[11] A possible reason for deviations can arise from differences in the host materials and guest concentration as well as approximations by the force field and the simulation methods. b) Simulated values of Θ as a function of the TDV direction δ.

For all emitters included in this study, we have used time-dependent density functional theory (TDDFT) calculations[32] of geometry-optimized triplet excitations to calculate the intramolecular TDV directions. These first-principles calculations predict a TDV direction within the ligand plane with a negative angle δ (as defined in the inset of **Figure 8a**) between -17° and -36°. In the main part of **Figure 8a**, we show the resulting Θ values. The orientation distribution of the TDV directions is shown in **Figure S3**. For the three systems studied already in **Figure 1**, the Θ values as obtained from the TDDFT calculations are larger than those given in **Figure 1**. These were obtained using $\delta \cong +20°$, based on a rough estimation from experiments on a single crystal of Re(ppy)(CO)$_4$.[33] Nevertheless, the predicted and experimental trends are still similar: only the system CPB:(Ir(bppo)$_2$(acac) shows a significantly reduced Θ value.

Figure 8b shows for all systems studied in this work the influence of δ on the Θ value over the interval between $\delta = -30°$ to $\delta = +30°$. Using the θ-values as obtained for this interval from the TDDFT calculations as a possible uncertainty-range, the simulation results would predict that apart from the CPB:(Ir(bppo)$_2$(acac) system only the TCTA:Ir(ppy)$_2$(acac) system (Θ = 0.29) shows a significant deviation from Θ = 1/3. For Ir(ppy)$_2$(acac) in CBP and in a 1:1 mixed host of TCTA and B3PYMPM, indeed a reduced value of Θ (in the range 0.22 to 0.24) has been found.[9, 11]

8. Conclusions

The orientation distribution of (dye-)molecules in OLEDs is important because an anisotropic orientation of transition dipole moments directly influences the light-outcoupling efficiency, and thus the device efficiency. Nonetheless, its molecular origin is not well understood. We have demonstrated that our Monte Carlo based molecular simulation method mimicking the vapor deposition process allows a quantitative analysis of the orientation of (dye-) molecules and yields results which are in agreement with experimental data. We find that the short-range van der Waals interaction between the phosphorescent dye molecules and other molecules at the film surface is responsible for the orientation. The electrostatic dipole-dipole interaction with the other molecules slightly reduces the anisotropy strength. While only few materials studied in this work show an improved outcoupling efficiency, almost all of them (including the host materials) show a significant orientation anisotropy which, in combination with the electrostatic dipole moments of the molecules, leads to a modified internal electric field which will influence the charge transport and recombination processes. The simulation methods demonstrated in this work can help to systematically explore the chemical space while searching for dye molecules with improved outcoupling efficiency.

ASSOCIATED CONTENT

Supporting Information. Distance-dependent κ-distributions, TDDFT results of the TDV direction and orientation distributions of the TDV. This material is available free of charge via the Internet at http://pubs.acs.org.

AUTHOR INFORMATION

Corresponding Author

* wolfgang.wenzel@kit.edu

Author Contributions

The manuscript was written through contributions of all authors. All authors have given approval to the final version of the manuscript.

Funding Sources

- EU Horizon2020 projects EXTMOS (Grant Number: 646176) and MOSTOPHOS (Grant Number 646259)
- Dutch-German project MODEOLED: Funding by the Dutch Technology Foundation STW, the applied science division of NWO, and the Technology Program of the Dutch Ministry of Economic Affairs (Project No. 12200) as well as "Deutsche Forschungsgemeinschaft" (DFG; Project No. WE1863/22-1)
- High Performance Computing 2 program of the Baden-Württemberg Stiftung (Project "Multi-Skalen-Modellierung von Materialien und Bauelementen für die Energieumwandlung und Energiespeicherung")
- This work was performed on the computational resource ForHLR I funded by the Ministry of Science, Research and the Arts Baden-Württemberg and the DFG ("Deutsche Forschungsgemeinschaft").

ACKNOWLEDGMENT

The authors acknowledge funding by the EU Horizon2020 projects EXTMOS (Grant Number: 646176) and MOSTOPHOS (Grant Number 646259), the Dutch-German project MODEOLED, and the High Performance Computing 2 program of the Baden-Württemberg Stiftung (Project "Multi-Skalen-Modellierung von Materialien und Bauelementen für die Energieumwandlung und Energiespeicherung"). On the Dutch side, the MODEOLED project is supported by the Dutch Technology Foundation STW, the applied science division of NWO, and the Technology Program of the Dutch Ministry of Economic Affairs (Project No. 12200). On the German side, it is supported by the "Deutsche Forschungsgemeinschaft" (DFG; Project No. WE1863/22-1). This work was performed on the computational resource ForHLR I funded by the Ministry of Science, Research and the Arts Baden-Württemberg and the DFG ("Deutsche Forschungsgemeinschaft").

REFERENCES

1. Schmidt, T. D.; Setz, D. S.; Flämmich, M.; Frischeisen, J.; Michaelis, D.; Krummacher, B. C.; Danz, N.; Brütting, W., Evidence for non-isotropic emitter orientation in a red phosphorescent organic light-emitting diode and its implications for determining the emitter's radiative quantum efficiency. *Appl. Phys. Lett.* **2011,** 99, (16), 225.
2. Murawski, C.; Elschner, C.; Lenk, S.; Reineke, S.; Gather, M. C. In *Orientation of OLED Emitter Molecules Revealed by XRD*, Solid-State Lighting, 2016; Optical Society of America: 2016; p SSW2D. 7.
3. Jeon, S. O.; Jang, S. E.; Son, H. S.; Lee, J. Y., External quantum efficiency above 20% in deep blue phosphorescent organic Light-Emitting diodes. *Adv. Mater. (Weinheim, Ger.)* **2011,** 23, (12), 1436-1441.
4. Reineke, S.; Rosenow, T. C.; Lüssem, B.; Leo, K., Improved High-Brightness Efficiency of Phosphorescent Organic LEDs Comprising Emitter Molecules with Small Permanent Dipole Moments. *Adv. Mater. (Weinheim, Ger.)* **2010,** 22, (29), 3189-3193.
5. Lee, J.; Chen, H.-F.; Batagoda, T.; Coburn, C.; Djurovich, P. I.; Thompson, M. E.; Forrest, S. R., Deep blue phosphorescent organic light-emitting diodes with very high brightness and efficiency. *Nat. Mater.* **2015,** advance online publication.
6. Lampe, T.; Schmidt, T. D.; Jurow, M. J.; Djurovich, P. I.; Thompson, M. E.; Brütting, W., Dependence of phosphorescent emitter orientation on deposition technique in doped organic films. *Chem. Mater.* **2016,** 28, (3), 712-715.
7. Jurow, M. J.; Mayr, C.; Schmidt, T. D.; Lampe, T.; Djurovich, P. I.; Brütting, W.; Thompson, M. E., Understanding and predicting the orientation of heteroleptic phosphors in organic light-emitting materials. *Nat. Mater.* **2016,** 15, (1), 85-91.
8. Mayr, C.; Schmidt, T. D.; Brütting, W., High-efficiency fluorescent organic light-emitting diodes enabled by triplet-triplet annihilation and horizontal emitter orientation. *Appl. Phys. Lett.* **2014,** 105, (18), 168_1.
9. Liehm, P.; Murawski, C.; Furno, M.; Lüssem, B.; Leo, K.; Gather, M. C., Comparing the emissive dipole orientation of two similar phosphorescent green emitter molecules in highly efficient organic light-emitting diodes. *Appl. Phys. Lett.* **2012,** 101, (25), 253304.
10. Flämmich, M.; Frischeisen, J.; Setz, D. S.; Michaelis, D.; Krummacher, B. C.; Schmidt, T. D.; Brütting, W.; Danz, N., Oriented phosphorescent emitters boost OLED efficiency. *Organic Electronics* **2011,** 12, (10), 1663-1668.
11. Kim, K. H.; Moon, C. K.; Lee, J. H.; Kim, S. Y.; Kim, J. J., Highly Efficient Organic Light-Emitting Diodes with Phosphorescent Emitters Having High Quantum Yield and Horizontal Orientation of Transition Dipole Moments. *Adv. Mater. (Weinheim, Ger.)* **2014,** 26, (23), 3844-3847.
12. Kim, S. Y.; Jeong, W. I.; Mayr, C.; Park, Y. S.; Kim, K. H.; Lee, J. H.; Moon, C. K.; Brütting, W.; Kim, J. J., Organic Light-Emitting diodes with 30% external quantum efficiency based on a horizontally oriented emitter. *Adv. Funct. Mater.* **2013,** 23, (31), 3896-3900.
13. Lee, J. H.; Sarada, G.; Moon, C. K.; Cho, W.; Kim, K. H.; Park, Y. G.; Lee, J. Y.; Jin, S. H.; Kim, J. J., Finely Tuned Blue Iridium Complexes with Varying Horizontal Emission Dipole Ratios and Quantum Yields for Phosphorescent Organic Light-Emitting Diodes. *Advanced Optical Materials* **2015,** 3, (2), 211-220.
14. Kim, K.-H.; Lee, S.; Moon, C.-K.; Kim, S.-Y.; Park, Y.-S.; Lee, J.-H.; Lee, J. W.; Huh, J.; You, Y.; Kim, J.-J., Phosphorescent dye-based supramolecules for high-efficiency organic light-emitting diodes. *Nature communications* **2014,** 5, 4769.
15. Ito, E.; Washizu, Y.; Hayashi, N.; Ishii, H.; Matsuie, N.; Tsuboi, K.; Ouchi, Y.; Harima, Y.; Yamashita, K.; Seki, K., Spontaneous buildup of giant surface potential by vacuum deposition of Alq 3 and its removal by visible light irradiation. *J. Appl. Phys.* **2002,** 92, (12), 7306-7310.
16. Noguchi, Y.; Miyazaki, Y.; Tanaka, Y.; Sato, N.; Nakayama, Y.; Schmidt, T. D.; Brütting, W.; Ishii, H., Charge

accumulation at organic semiconductor interfaces due to a permanent dipole moment and its orientational order in bilayer devices. *J. Appl. Phys.* **2012,** 111, (11), 114508.

17. Noguchi, Y.; Sato, N.; Miyazaki, Y.; Ishii, H., Light-and ion-gauge-induced space charges in tris-(8-hydroxyquinolate) aluminum-based organic light-emitting diodes. *Appl. Phys. Lett.* **2010,** 96, (14), 143305.

18. Neumann, T.; Danilov, D.; Lennartz, C.; Wenzel, W., Modeling disordered morphologies in organic semiconductors. *J. Comput. Chem.* **2013,** 34, (31), 2716-2725.

19. Stewart, J. J. P., MOPAC: a semiempirical molecular orbital program. *J. Comput.-Aided Mol. Des.* **1990,** 4, (1), 1-103.

20. Stewart, J. J., Optimization of parameters for semiempirical methods VI: more modifications to the NDDO approximations and re-optimization of parameters. *Journal of molecular modeling* **2013,** 19, (1), 1-32.

21. Becke, A. D., A new mixing of Hartree-Fock and local density-functional theories. *J. Chem. Phys.* **1993,** 98, (2), 1372-1377.

22. Grimme, S.; Antony, J.; Ehrlich, S.; Krieg, H., A consistent and accurate ab initio parametrization of density functional dispersion correction (DFT-D) for the 94 elements H-Pu. *J. Chem. Phys.* **2010,** 132, (15), 154104.

23. Ahlrichs, R.; Bär, M.; Häser, M.; Horn, H.; Kölmel, C., Electronic structure calculations on workstation computers: The program system turbomole. *Chem. Phys. Lett.* **1989,** 162, (3), 165-169.

24. Schafer, A.; Horn, H.; Ahlrichs, R., Fully optimized contracted Gaussian basis sets for atoms Li to Kr. *J. Chem. Phys.* **1992,** 97, (4), 2571-2577.

25. Adachi, C.; Baldo, M. A.; Forrest, S. R.; Thompson, M. E., High-efficiency organic electrophosphorescent devices with tris (2-phenylpyridine) iridium doped into electron-transporting materials. *Appl. Phys. Lett.* **2000,** 77, (6), 904-906.

26. Kordt, P.; Andrienko, D., Modeling of Spatially Correlated Energetic Disorder in Organic Semiconductors. *J. Chem. Theory Comput.* **2015,** 12, (1), 36-40.

27. Strohriegl, P.; Wagner, D.; Schrögel, P.; Hoffmann, S. T.; Köhler, A.; Heinemeyer, U.; Münster, I.; Lennartz, C. In *Novel host materials for blue phosphorescent OLEDs*, Proc. SPIE, 2013; 2013; p 882906.

28. Moon, C.-K.; Kim, K.-H.; Kim, J.-J. In *Unraveling the origin of the orientation of Ir complexes doped in organic semiconducting layers*, Organic Light Emitting Materials and Devices XXI, 2017; International Society for Optics and Photonics: 2017; p 1036213.

29. Lee, T.; Caron, B.; Stroet, M.; Huang, D. M.; Burn, P. L.; Mark, A. E., The molecular origin of anisotropic emission in an organic light-emitting diode. *Nano Lett.* **2017**.

30. Mayr, C.; Brütting, W., Control of molecular dye orientation in organic luminescent films by the glass transition temperature of the host material. *Chem. Mater.* **2015,** 27, (8), 2759-2762.

31. Schmidt, T. D.; Lampe, T.; Djurovich, P. I.; Thompson, M. E.; Brütting, W., Emitter Orientation as a Key Parameter in Organic Light-Emitting Diodes. *Physical Review Applied* **2017,** 8, (3), 037001.

32. Furche, F.; Rappoport, D., III. Density functional methods for excited States: Equilibrium structure and electronic spectra. *Theoretical and computational chemistry* **2005,** 16, 93-128.

33. Vanhelmont, F. W.; Strouse, G. F.; Güdel, H. U.; Stückl, A. C.; Schmalle, H. W., Synthesis, crystal structure, high-resolution optical spectroscopy, and extended Hückel calculations on cyclometalated [Re (CO) 4 (ppy)](ppy= 2-Phenylpyridine). *J. Phys. Chem. A* **1997,** 101, (16), 2946-2952.

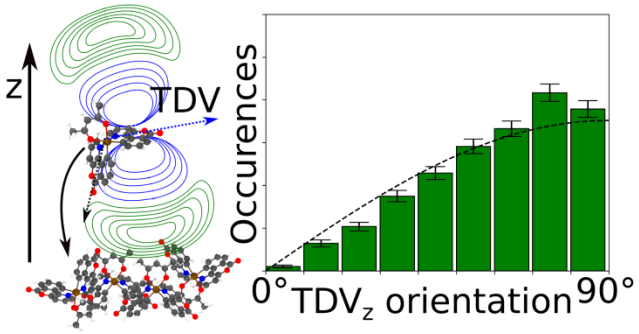
z
TDV
Occurences
0°
TDV$_z$ orientation
90°